Study of $B_c \to J/\psi\pi$, $\eta_c\pi$ decays with perturbative QCD approach

Junfeng Sun,[1,2] Dongsheng Du,[3] and Yueling Yang[1]

[1] *College of Physics and Information Engineering,*

Henan Normal University, Xinxiang 453007, China[*]

[2] *Theoretical Physics Center for Science Facilities,*

Chinese Academy of Sciences, P.O.Box 918(4), Beijing 100049, China

[3] *Institute of High Energy Physics, Chinese Academy of Sciences,*

P.O.Box 918(4), Beijing 100049, China

Abstract

The $B_c \to J/\psi\pi$, $\eta_c\pi$ decays are studied with the perturbative QCD approach. It is found that the form factors $A_{0,1,2}^{B_c \to J/\psi}$ and $F_0^{B_c \to \eta_c}$ for the $B_c \to J/\psi$, η_c transitions and the branching ratios are sensitive to the parameters ω, v, $f_{J/\psi}$ and f_{η_c}, where ω and v are the parameters of the charmonium wave functions for Coulomb potential and harmonic oscillator potential, respectively, $f_{J/\psi}$ and f_{η_c} are the decay constants of the J/ψ and η_c mesons, respectively. The large branching ratios and the clear signals of the final states make the $B_c \to J/\psi\pi$, $\eta_c\pi$ decays to be the prospective channels for measurements at the hadron colliders.

[*]Mailing address

arXiv:0808.3619v3 [hep-ph] 28 Feb 2009

I. INTRODUCTION

The Large Hadron Collider (LHC) is schedule to run in this year. At the era of the LHC, there is still a room for B physics. The study of the decays of B mesons is important and interesting for the determination of the flavor parameters of the Standard Model (SM), the exploration of CP violation, the search of new physics beyond SM, and so on. The decays of $B_{u,d}$ mesons have been investigated widely by the detectors at the e^+e^- colliders, such as the CLEO, Babar, Belle. The B_c meson could be produced abundantly and studied detailedly at the hadron colliders, such as the Tevatron and LHC. The study of the B_c mesons will highlight the advantages of B physics.

Compared with the $B_{u,d}$ mesons, the B_c mesons have some special properties: (1) The B_c mesons are the "double heavy-flavored" binding systems. We can study the two heavy flavors of both b and c quarks simultaneously with the B_c mesons. (2) The B_c mesons have much rich decay modes, because they have sufficiently large mass and that either b or c quarks can decay individually. The potential decays of the B_c mesons permit us to over-constrain quantities determined by the $B_{u,d}$ meson decays.

It is estimated that one could expect around 5×10^{10} B_c events per year at LHC [1]. The nonleptonic decays of the B_c mesons have been studied in previous literature [1, 2]. The theoretical status of the B_c meson was reviewed in [1]. In this paper, we will concentrate on the $B_c \to J/\psi\pi$, $\eta_c\pi$ decays using the perturbative QCD approach. There are several reasons :

(i) From the experimental point of view, the decay modes containing the signal of J/ψ meson are among the most easily reconstructible B_c decay modes, due to the narrow-peak of J/ψ and the high purity $J/\psi \to \ell^+\ell^-$. For example, the B_c mesons are firstly discovered via $B_c \to J/\psi\ell\nu$ by the CDF Collaboration in 1998 [3]. Recently the CDF and D0 Collaborations announced their accurate measurements on the B_c mesons via $B_c \to J/\psi\pi$ mode [4, 5]. Especially, compared with the semi-leptonic decays where the neutrino momentum is not detected directly, all final-state particles are detectable for the $B_c \to J/\psi\pi$, $\eta_c\pi$ decays. It is estimated that the ATLAS detector would be able to record about 5600 events of $B_c \to J/\psi\pi$ per year [1]. So $B_c \to J/\psi\pi$, $\eta_c\pi$ decays may be two of the most prospective channels for measurements.

(ii) From the phenomenological point of view: In recent years, several attractive methods have been proposed to study the nonleptonic B decays, such as the QCD factorization [6], perturbative QCD method (pQCD) [7, 8, 9], soft and collinear effective theory [10, 11], and so on. The study of B_c decays provides opportunities to test the k_T and collinear factorizations, to check the various treatments for the entanglement of different energy modes, to deepen our understanding on perturbative and nonperturbative contributions. These methods developed recently are widely applied to the nonleptonic two-body $B_{u,d,s}$ decays in literature, but with very few application of these methods on the B_c meson decays. The appealing feature of the pQCD factorization [7, 8, 9] is that form factors can be computed in terms of wave functions (nonperturbative contributions) and hard kernels (perturbative contributions arising from hard gluon exchange) assuming that additional soft contributions are suppressed by the Sudakov factor in the heavy quark limit. Although there is still some controversy about the pQCD method, for example, the problem of gauge invariant [12], the pQCD method has been extensively used in the past to study nonleptonic B decays with fairly good phenomenological results [13]. In this paper, we will take the $B_c \rightarrow J/\psi\pi$, $\eta_c\pi$ decays as examples to discuss the B_c decays in the perturbative QCD method.

(iii) From the theoretical point of view: The $B_c \rightarrow J/\psi\pi$, $\eta_c\pi$ decays are similar to the $B_q \rightarrow D_q^{(*)}\pi$ (where $q = u$, d, s) decays with the "spectator quark" ansatz. The $B_q \rightarrow D_q^{(*)}\pi$ decays have been studied with the pQCD method [15]. Compared with the $B_q \rightarrow D_q^{(*)}\pi$ decays, the $B_c \rightarrow J/\psi\pi$, $\eta_c\pi$ decays are easy to deal with because that the B_c meson and the J/ψ (or η_c) meson are heavy quarkonia and could be described approximatively by nonrelativistic dynamics. Given $m_{B_c} \simeq m_b + m_c$, the wave function of the B_c mesons would be close to $\delta(x - m_c/m_{B_c})$ in the nonrelativistic limit (where m_{B_c}, m_b, and m_c are the masses of the B_c mesons, b quark, and c quark, respectively; x denotes the momentum fraction of the c quark in the B_c meson). The wave functions for pion are well-defined. The only parameter is the wave function of the J/ψ (or η_c) meson. So the $B_c \rightarrow J/\psi\pi$, $\eta_c\pi$ decays provide good platform to test quark potential models derived from QCD.

This paper is organized as follows: In Section II, we discuss the theoretical framework and compute the decay amplitudes for $B_c \rightarrow J/\psi\pi$, $\eta_c\pi$ with the perturbative QCD approach.

The section III is devoted to the numerical results. Finally, we summarize in Section IV.

II.   THEORETICAL FRAMEWORK AND THE DECAY AMPLITUDES

A.   The effective Hamiltonian

Using the operator product expansion and renormalization group (RG) equation, the low energy effective Hamiltonian for $B_c \to X_{c\bar{c}}\pi$ decay can be written as (where $X_{c\bar{c}} = J/\psi,\ \eta_c$):

$$\mathcal{H}_{eff} = \frac{G_F}{\sqrt{2}} V_{cb} V_{ud}^* \big\{ C_1(\mu) Q_1 + C_2(\mu) Q_2 \big\} + \text{H.c.}, \tag{1}$$

where $V_{cb} V_{ud}^*$ is the CKM factor accounting for the strengths of the concerned nonleptonic decay processes. The parameters $C_i(\mu)$ are Wilson coefficients which have been evaluated to the next-to-leading order with the perturbation theory. The expressions of the local operators are

$$Q_1 = [\bar{c}_\alpha \gamma_\mu (1 - \gamma_5) b_\alpha][\bar{d}_\beta \gamma^\mu (1 - \gamma_5) u_\beta], \qquad Q_2 = [\bar{c}_\alpha \gamma_\mu (1 - \gamma_5) b_\beta][\bar{d}_\beta \gamma^\mu (1 - \gamma_5) u_\alpha], \tag{2}$$

where α, β are color indices. The essential problem obstructing the calculation of decay amplitude is how to evaluate the hadronic matrix elements of the local operators.

B.   Hadronic matrix elements

The calculation of the hadronic matrix elements is difficult due to the nonperturbative effects arising from the strong interactions. Phenomenologically, the simplest approach to hadronic matrix elements is the Bauer-Stech-Wirbel (BSW) model [14] based on color transparency and naive factorization hypothesis, where the hadronic matrix elements are parameterized into the product of the decay constants and the transition form factors. One defect of the rough BSW method is that the hadronic matrix elements cannot cancel the renormalization scheme- and scale- dependence of the Wilson coefficients. To remedy this problem, the "nonfactorizable" contributions must be taken into account. Using the Brodsky-Lepage approach [16], the hadronic matrix elements can be written as the convolution of a hard-scattering amplitude, including some perturbative QCD contributions, and meson wave functions.

Recently, a modified perturbative QCD formalism has been proposed under the k_T factorization framework [7, 8, 9]. The Sudakov effects are introduced to modify the endpoint behavior. The decay amplitudes are factorized into three convolution factors: the "harder" functions, the heavy quark decay subamplitudes, and the nonperturbative meson wave functions, which are characterized by the $W^\pm$ boson mass m_W, the typical scale t of the decay processes, and the hadronic scale Λ_{QCD}, respectively. Using the resummation technique and the RG treatment, the final decay amplitudes can be expressed as

$$\mathcal{A}(B_c \to X_{c\bar{c}}\pi) \propto C(t) \otimes H(t) \otimes \Phi_{B_c}(x_1, b_1) \otimes \Phi_{X_{c\bar{c}}}(x_2, b_2) \otimes \Phi_\pi(x_3, b_3), \tag{3}$$

where the Wilson coefficient $C(t)$ is calculated in perturbative theory at scale of m_W and evolved down to the typical scale t using the RG equations, $\otimes$ denotes the convolution over parton kinematic variables, $H(t)$ is the hard-scattering subamplitude, the wave functions $\Phi(x, b)$ absorb nonperturbative long-distance dynamics, x is the longitudinal momentum fraction of the valence quark of the meson, b is the conjugate variable of the transverse momentum of the valence quark of the meson. According the arguments in [7, 8, 9], the amplitude of Eq.(3) is free from the renormalization scale dependence.

C. Kinematic variables

For convenience, the kinematics variables are described in the terms of the light cone coordinate. The momenta of the valence quarks and hadrons in the rest frame of the B_c meson are defined by

$$
\begin{aligned}
p_1 &= \tfrac{m_{B_c}}{\sqrt{2}}(1, 1, \vec{0}_\perp), & k_1 &= x_1 p_1, & n_2 &= (1, 0, 0), \\
p_2 &= \tfrac{m_{B_c}}{\sqrt{2}}(1, r_{X_{c\bar{c}}}^2, \vec{0}_\perp), & k_2 &= x_2 p_2 + (0, 0, \vec{k}_{2\perp}), & \epsilon_\parallel &= \tfrac{1}{\sqrt{2}r_\psi}(1, -r_\psi^2, \vec{0}), \\
p_3 &= \tfrac{m_{B_c}}{\sqrt{2}}(0, 1 - r_{X_{c\bar{c}}}^2, \vec{0}_\perp), & k_3 &= x_3 p_3 + (0, 0, \vec{k}_{3\perp}), & n_3 &= (0, 1, 0),
\end{aligned}
$$

where the notation of momenta of p_i and k_i are displayed in FIG.1. The null vectors n_2 and n_3 are the plus and minus directions, respectively. The mass of the π meson is neglected. The momentum of the π meson is chosen to be parallel to the null vector n_3. The mass ratios are $r_{X_{c\bar{c}}} = m_{X_{c\bar{c}}}/m_{B_c}$, $r_b = m_b/m_{B_c}$, $r_c = m_c/m_{B_c}$.

D. Bilinear operator matrix elements for mesons

In terms of the notation in [17], the nonlocal bilinear-quark operator matrix elements associated with the B_c meson, π meson, the longitudinally polarized J/ψ meson, η_c meson are decomposed into [17, 18]

$$\langle 0|\bar{c}_\alpha(z)b_\beta(0)|B_c^-(p_1)\rangle = \frac{+i}{\sqrt{2N_c}}\int \mathbf{d}^4 k_1\, \mathrm{e}^{-ik_1\cdot z}\Big[\big(\not{p}_1+m_{B_c}\big)\gamma_5\phi_{B_c}(k_1)\Big]_{\beta\alpha}, \tag{4}$$

$$\begin{aligned}
&\langle \pi^-(p_3)|\bar{d}_\alpha(0)u_\beta(z)|0\rangle \\
&= \frac{-i}{\sqrt{2N_c}}\int_0^1 \mathbf{d}x_3\, \mathrm{e}^{+ix_3 p_3 z}\Big\{\gamma_5\Big[\,\not{p}_3\phi_\pi^a(x_3)+\mu_\pi\phi_\pi^p(x_3)-\mu_\pi(\not{n}_3\not{n}_2-n_3\cdot n_2)\phi_\pi^t(x_3)\Big]\Big\}_{\beta\alpha},
\end{aligned} \tag{5}$$

$$\langle J/\psi(p_2,\epsilon_\|)|\bar{c}_\alpha(0)c_\beta(z)|0\rangle = \frac{1}{\sqrt{2N_c}}\int \mathbf{d}^4 k_2\, \mathrm{e}^{+ik_2\cdot z}\,\not{\epsilon}_\|\Big[m_{J/\psi}\phi_\psi^L(k_2)+\not{p}_2\phi_\psi^t(k_2)\Big]_{\beta\alpha}, \tag{6}$$

$$\langle \eta_c(p_2)|\bar{c}_\alpha(0)c_\beta(z)|0\rangle = \frac{-i}{\sqrt{2N_c}}\int \mathbf{d}^4 k_2\, \mathrm{e}^{+ik_2\cdot z}\Big\{\gamma_5\Big[\,\not{p}_2\phi_{\eta_c}^v(k_2)+m_{\eta_c}\phi_{\eta_c}^s(k_2)\Big]\Big\}_{\beta\alpha}, \tag{7}$$

where the wave functions ϕ_π^a, ϕ_ψ^L, $\phi_{\eta_c}^v$ are twist-2, ϕ_π^p, ϕ_π^t, ϕ_ψ^t, $\phi_{\eta_c}^s$ are twist-3, $\mu_\pi = m_\pi^2/(m_u + m_d)$. Their expressions are collected in APPENDIX A and B.

For the wave function ϕ_{B_c}, we will take the nonrelativistic approximation as stated in the introduction, i.e.

$$\phi_{B_c} = \frac{f_{B_c}}{2\sqrt{2N_c}}\delta(x - r_c), \tag{8}$$

where N_c is the color number, f_{B_c} is the decay constant of the B_c meson.

E. $B_c \rightarrow X_{c\bar{c}}$ form factors

The $B_c \rightarrow X_{c\bar{c}}$ form factors are defined as [14, 19]:

$$\begin{aligned}
&\langle \eta_c(p_2)|\bar{c}\gamma^\mu b|B_c(p_1)\rangle \\
&= \frac{m_{B_c}^2 - m_{\eta_c}^2}{q^2}q^\mu F_0^{B_c\to\eta_c}(q^2) + \Big[(p_1 + p_2)^\mu - \frac{m_{B_c}^2 - m_{\eta_c}^2}{q^2}q^\mu\Big]F_1^{B_c\to\eta_c}(q^2),
\end{aligned} \tag{9}$$

$$\begin{aligned}
&\langle J/\psi(p_2,\epsilon)|\bar{c}\gamma^\mu\gamma_5 b|B_c(p_1)\rangle \\
&= +i\frac{(\epsilon^*\cdot q)}{q^2}2m_{J/\psi}q^\mu A_0^{B_c\to J/\psi}(q^2) + i\epsilon^{*\mu}(m_{B_c}+m_{J/\psi})A_1^{B_c\to J/\psi}(q^2) \\
&\quad -i\frac{(\epsilon^*\cdot q)}{m_{B_c}+m_{J/\psi}}(p_1 + p_2)^\mu A_2^{B_c\to J/\psi}(q^2) - i\frac{(\epsilon^*\cdot q)}{q^2}2m_{J/\psi}q^\mu A_3^{B_c\to J/\psi}(q^2),
\end{aligned} \tag{10}$$

where $q = p_1 - p_2$, ϵ^* denotes the polarization vector of the J/ψ meson. $F_{0,1}^{B_c\to\eta_c}$ and $A_{0,1,2,3}^{B_c\to J/\psi}$ are the transition form factors. In addition, at large recoil limit, $q^2 = 0$, we have

$$F_0^{B_c\to\eta_c}(0) = F_1^{B_c\to\eta_c}(0), \qquad A_0^{B_c\to J/\psi}(0) = A_3^{B_c\to J/\psi}(0), \tag{11}$$

$$A_3^{B_c \to J/\psi}(q^2) = \frac{m_{B_c}+m_{J/\psi}}{2m_{J/\psi}} A_1^{B_c \to J/\psi}(q^2) - \frac{m_{B_c}-m_{J/\psi}}{2m_{J/\psi}} A_2^{B_c \to J/\psi}(q^2). \tag{12}$$

In the perturbative QCD approach, these form factors can be generally written as

$$A_i^{B_c \to J/\psi} \text{ (or } F_i^{B_c \to \eta_c}) \propto \Phi_{B_c}(x_1, b_1) \otimes H(t) \otimes \Phi_{X_{c\bar{c}}}(x_2, b_2). \tag{13}$$

At large recoil region, the $B_c \to X_{c\bar{c}}$ transition is dominated by the single gluon exchange as depicted FIG.2. The expressions for $F_0^{B_c \to \eta_c}$ and $A_{1,2}^{B_c \to J/\psi}$ are listed in APPENDIX C.

F. The decay amplitudes

The $B_c \to J/\psi\pi$, $\eta_c\pi$ decays are tree dominated within the framework of Operator Product Expansion, and without pollution from penguins and annihilation diagrams. In the perturbative QCD approach, the Feynman diagrams are shown in FIG.3, where (a) and (b) are factorizable topology, (c) and (d) are nonfactorizable topology. After a straightforward calculation using the modified perturbative QCD formalism Eq.(3), we obtain the decay amplitudes

$$\mathcal{A}(B_c^- \to X_{c\bar{c}}\pi^-) = \frac{G_F}{\sqrt{2}} V_{cb}V_{ud}^* \sum_{i=a,b,c,d} \mathcal{A}_{\text{FIG.3(i)}}, \tag{14}$$

where the CKM matrix elements $V_{cb}V_{ud}^* = A\lambda^2(1-\lambda^2/2-\lambda^4/8) + \mathcal{O}(\lambda^8)$ with the Wolfenstein parameterization. The detailed expressions of $\mathcal{A}_{\text{FIG.3(i)}}$ are shown in APPENDIX D. From the expressions, we can clearly see that only the twist-2 distribution amplitude of the π meson contribute to the decay amplitudes.

III. NUMERICAL RESULTS AND DISCUSSIONS

The branching ratios in the B_c meson rest frame can be written as:

$$\mathcal{BR}(B_c \to X_{c\bar{c}}\pi) = \frac{\tau_{B_c}}{8\pi} \frac{|p|}{m_{B_c}^2} |\mathcal{A}(B_c \to X_{c\bar{c}}\pi)|^2, \tag{15}$$

where the common momentum $|p| = (m_{B_c}^2 - m_{X_{c\bar{c}}}^2)/2m_{B_c}$, the lifetime and mass of the B_c meson are $m_{B_c} = 6.276 \pm 0.004$ GeV and $\tau_{B_c} = 0.46 \pm 0.07$ ps [20], respectively. Other input parameters are

$m_c = 1.5$ GeV, $\qquad m_{J/\psi} = 3096.916 \pm 0.011$ MeV [20], $\quad f_{J/\psi} = 405 \pm 14$ MeV [18],

$m_b = 4.20^{+0.17}_{-0.07}$ GeV [20], $\quad m_{\eta_c} = 2980.3 \pm 1.2$ MeV [20], $\qquad f_{\eta_c} = 420 \pm 50$ MeV [18],

$A = 0.814^{+0.021}_{-0.022}$ [20], $\qquad \lambda = 0.2257^{+0.0009}_{-0.0010}$ [20], $\qquad f_{B_c} = 489 \pm 4$ MeV [21].

If not specified explicitly, we shall take their central values as the default input.

Our numerical results [a] on the form factors $F_0^{B_c \to \eta_c}$ and $A_{0,1,2}^{B_c \to J/\psi}$ are listed in TABLE.I, where ω and v are the parameters in the wave functions of Eqs.(B7)-(B10) and Eqs.(B17)-(B20), respectively. From the numbers in TABLE.I, we can see that

(i) The form factors F_0 and $A_{0,1,2}$ decrease with the increasing parameters ω and v. The form factors of F_0 and $A_{0,1}$ are more sensitive to the parameters ω or/and v than the form factor of A_2. Uncertainties of form factors F_0 and $A_{0,1}$ subjected to the charmonium wave function for Coulomb potential are larger than those for harmonic oscillator potential. Uncertainties of F_0 and $A_{0,1}$ related to the parameters ω in our given range are about $16\% \sim 20\%$, while those related to the parameters v in our given range are about $20\% \sim 30\%$. In addition, the uncertainties of the decay constants f_{B_c}, $f_{J/\psi}$ and f_{η_c} will bring $\sim 0.8\%$, 3% and 12% uncertainties to the form factors F_0 and $A_{0,1,2}$, respectively.

(ii) The form factors have been widely studied in the previous works [22, 23, 24, 25, 26, 27, 28, 29, 30, 31, 32]. There are large difference among the predictions in respect of various approaches. Compared with the previous results where $F_0^{B_c \to \eta_c} \approx A_{0,1,2}^{B_c \to J/\psi}$ [22, 25, 26, 27, 28, 29, 31, 32], our numerical results show that $F_0^{B_c \to \eta_c} \approx A_0^{B_c \to J/\psi} > A_1^{B_c \to J/\psi} > A_2^{B_c \to J/\psi}$. With some appropriate parameters, our results [b] on the form factors F_0 and $A_{0,1}$ are in agreement with those in the previous works [22, 25, 26, 27, 28, 29, 31, 32]. Our results on the form factors A_2 are smaller than those in the previous works [25, 26, 27, 28, 29, 31, 32]. According to the "spectator quark" ansatz, there might be $F_0^{B_c \to \eta_c}$ (or $A_{0,1,2}^{B_c \to J/\psi}$) $\sim F_0^{B \to D}$ (or $A_{0,1,2}^{B \to D^*}$) ≈ 0.6 by intuition. So maybe the results based on the three-point QCD sum rules [23, 24] are small.

Our numerical results on the amplitudes and branching ratios for $B_c \to J/\psi\pi$, $\eta_c\pi$ decays

---

[a] Here, we think that theoretical prediction on input parameters, such as ω and v, relies on our educated guesswork. All values within allowed ranges should be treated on an equal footing, irrespective of how close they are from the edges of the allowed range. For example, we cannot say that the probability of $\omega = 0.5$ GeV is less than that of $\omega = 0.6$ GeV, while the error means the usual one standard deviation in the form of $A_{-\delta A}^{+\delta A}$ (such as the expression of $m_{B_c} = 6.276 \pm 0.004$ GeV). So our numerical results had better to be given by a range to show the theoretical uncertainties, rather than the form of $A_{-\delta A}^{+\delta A}$.

[b] For example, $F_0^{B_c \to \eta_c} = 0.430$ (0.464), $A_0^{B_c \to J/\psi} = 0.446$ (0.470), $A_1^{B_c \to J/\psi} = 0.392$ (0.427) for $v = 0.80$ ($\omega = 1.60$ GeV).

are listed in TABLE.II and III. From the numbers in TABLE.II and III, we can see that

(i) The contributions of the nonfactorizable topology [FIG.3 (c) and (d)] can provide large strong phases. The strong phases of the FIG.3 (c) topology $\delta \gtrsim 110°$, while the strong phases of the FIG.3 (d) topology $\delta \lesssim -50°$. The interferences between FIG.3 (c) and (d) are destructive. The strong phases from nonfactorizable topology decrease with the increasing parameters ω and v. They are free from the uncertainties of the decay constants f_{B_c}, $f_{J/\psi}$ and f_{η_c}. The strong phases subjected to the charmonium wave function for Coulomb potential are larger than those for harmonic oscillator potential in our given ranges.

(ii) The dominated contributions to the branching ratios come from the factorizable topology [FIG.3 (a) and (b)]. The ratio of amplitudes $|\mathcal{A}_{\text{FIG.3(c+d)}}/\mathcal{A}_{\text{FIG.3(a+b)}}| \sim 1\%$ for $B_c \rightarrow J/\psi\pi$ decay, and about $2\% \sim 3\%$ for $B_c \rightarrow \eta_c\pi$ decay. The dominating amplitudes $\mathcal{A}_{\text{FIG.3(a,b)}}$ and the branching ratios decrease with the increasing parameters ω and v. Besides the large uncertainties from the parameter ω and v, the uncertainties of the decay constants $f_{J/\psi}$ and f_{η_c} will bring $\sim 7\%$ and $\sim 24\%$ uncertainties to the branching ratio for $B_c \rightarrow J/\psi\pi$ and $\eta_c\pi$ decays, respectively. Considered the uncertainties from the input parameters, our results on the branching ratios are basically consistent with those in previous works [31, 36, 37, 38, 41, 42, 43] (see the numbers in TABLE.IV). Compared with the results in [27, 29] where small form factors are used (see the numbers in TABLE.I), we find that our predictions are large. If with the same factor factors, our results generally agree with those in [27, 29]. The large predictions in [40] are obtained by the relations among the amplitudes under the quark diagram scheme, i.e. $\mathcal{A}(B_c \rightarrow \eta_c\pi) = V_{cb}/V_{ub}\mathcal{A}(B \rightarrow D_s\pi)$ and $\mathcal{A}(B_c \rightarrow J/\psi\pi) = V_{cb}/V_{ub}\mathcal{A}(B \rightarrow D_s\rho)$. Intuitively, the distribution amplitudes of the heavy quarkonia (such as B_c, J/ψ and η_c mesons) should be narrower than those of the "heavy-light" systems (such as B and D mesons). So, the superposition among the $B_c - J/\psi(\eta_c) - \pi$ systems might be less than those among the $B - D_s - \pi(\rho)$ systems, i.e. there might be $\mathcal{A}(B_c \rightarrow \eta_c\pi) \lesssim V_{cb}/V_{ub}\mathcal{A}(B \rightarrow D_s\pi)$ and $\mathcal{A}(B_c \rightarrow J/\psi\pi) \lesssim V_{cb}/V_{ub}\mathcal{A}(B \rightarrow D_s\rho)$. If this argument or/and assumption is true, then it is expected that the results in [40] would become smaller and be consistent with ours.

(iii) The dominating amplitudes $\mathcal{A}_{\text{FIG.3(a,b)}}$ and the branching ratios subjected to the char-

monium wave function for Coulomb potential are larger than those for harmonic oscillator potential. For a fixed value of parameter ω or v, the relation of the branching ratios is $\mathcal{BR}(B_c \to \eta_c \pi) \gtrsim \mathcal{BR}(B_c \to J/\psi \pi)$. There are at least two reasons, one is that the phase spaces for $B_c \to \eta_c \pi$ decay is larger than those for $B_c \to J/\psi \pi$ decay, the other is that $F_0^{B_c \to \eta_c} \gtrsim A_0^{B_c \to J/\psi}$ (see the numbers in TABLE.I). The relation of the branching ratios is in agreement with the previous predictions [22, 27, 29, 37, 38, 40, 41, 42, 43]. The signal of $B_c \to J/\psi \pi$ decay has been identified by the detectors at hadron collider Tevatron. It is eagerly expected that the signal of $B_c \to \eta_c \pi$ decay is at the near corner for Tevatron and LHC.

IV. SUMMARY AND CONCLUSION

In this paper, the $B_c \to J/\psi \pi$, $\eta_c \pi$ decays are studied with the perturbative QCD approach. It is found that the form factors $A_{0,1,2}^{B_c \to J/\psi}$ and $F_0^{B_c \to \eta_c}$ for the $B_c \to J/\psi$, η_c transitions and the branching ratios for $B_c \to J/\psi \pi$ and $\eta_c \pi$ decays, they decrease with the increasing parameters ω and v, where ω and v are the parameters of the charmonium wave functions for Coulomb potential and harmonic oscillator potential, respectively. Therefore, the $B_c \to J/\psi \pi$, $\eta_c \pi$ decay modes provide good places to test quark potential models. In addition, the large uncertainties come from the uncertainties of the decay constants $f_{J/\psi}$ and f_{η_c}, which could be reduced greatly with the more accurate experimental measurements or/and better theoretical calculations. There are some other uncertainties not considered here, such as the power suppressed terms, the high order corrections, the effects of the final states interaction, the relativistic corrections to the wave functions, the model dependencies of the wave functions, and so on. They might be important in some cases (for example, the chirally-enhanced power corrections to the $B \to \pi K$ decays are not much suppressed numerically.) and deserve the dedicated researches. So our results might be regarded as the estimations under the pQCD framework. One should not be too serious about these numbers. Anyway, the large branching ratios and the clear signals of the final states make the measurement of the interesting $B_c \to J/\psi \pi$, $\eta_c \pi$ decays easily at the hadron colliders.

APPENDIX A: WAVE FUNCTIONS OF THE π MESON

The distribution amplitude ϕ_π^a for the twist-2 wave function and the distribution amplitude ϕ_π^p and ϕ_π^t for the twist-3 wave functions are [17]

$$\phi_\pi^a(x) \;=\; \frac{f_\pi}{2\sqrt{2N_c}} 6x\bar{x}\Big\{1 + 0.44 C_2^{3/2}(\bar{x} - x) + 0.25 C_4^{3/2}(\bar{x} - x)\Big\}, \tag{A1}$$

$$\phi_\pi^p(x) \;=\; \frac{f_\pi}{2\sqrt{2N_c}}\Big\{1 + 0.43 C_2^{1/2}(\bar{x} - x) + 0.09 C_4^{1/2}(\bar{x} - x)\Big\}, \tag{A2}$$

$$\phi_\pi^t(x) \;=\; \frac{f_\pi}{2\sqrt{2N_c}}\Big\{C_1^{1/2}(\bar{x} - x) + 0.55 C_3^{1/2}(\bar{x} - x)\Big\}, \tag{A3}$$

with the decay constant $f_\pi = 130$ MeV. The Gegenbauer polynomials are defined by

$$C_1^{1/2}(z) = z, \qquad\qquad C_2^{1/2}(z) = \frac{1}{2}(3z^2 - 1),$$

$$C_3^{1/2}(z) = \frac{1}{2}(5z^3 - 3z), \qquad C_4^{1/2}(z) = \frac{1}{8}(35z^4 - 30z^2 + 3),$$

$$C_2^{3/2}(z) = \frac{3}{2}(5z^2 - 1), \qquad C_4^{3/2}(z) = \frac{15}{8}(21z^4 - 14z^2 + 1).$$

APPENDIX B: WAVE FUNCTIONS OF THE J/ψ AND η_c MESONS

The heavy quarkonium, such as $c\bar{c}$, similar to diatomic molecules, might be amenable to a Born-Oppenheimer treatment [c] [1]. Following the prescription in [18, 33], two forms of the wave functions corresponding to two different nonrelativistic potentials will be derived.

1. wave functions for harmonic oscillator potential

In the nuclear shell model, a more realistic description of the nucleons inside the atomic nucleus is given by the Woods-Saxon potential. The Schrödinger equation subjected to the Woods-Saxon potential cannot be solved analytically, and must be treated numerically, but the energy levels as well as other properties can be arrived at by approximating the model with a three-dimensional harmonic oscillator. The spectroscopy of the heavy quarkonium $c\bar{c}$ can be treated by this model. The quantum number $n_r L$ for the J/ψ and η_c mesons is $1S$,

---

[c] The heavy quark-antiquark pair is bound by the gluon and light-quark clouds. The heavy quarks correspond to the nuclei in diatomic molecules. The gluon and light-quark fields correspond to the electrons, and provide adiabatic potentials [1].

where n_r and L are the radial quantum number and the orbital angular momentum quantum number, respectively. (note : the energy spectrum of a three-dimensional harmonic oscillator is given by $E_{n_r L} = \{2(n_r - 1) + L + \frac{3}{2}\}\omega$.) The radial wave function of the corresponding Schrödinger state is given by

$$\psi_{n_r L}(r) = \psi_{1S}(r) \propto \exp(-\alpha^2 r^2/2), \tag{B1}$$

where $\alpha^2 = m_c \omega/2$, ω is the frequency of oscillations or the quantum of energy.

Applying the Fourier transform, the state Eq.(B1) is replaced by the mapping representation on the momentum space,

$$\psi_{1S}(\vec{k}) \sim \int \mathbf{d}^3\vec{r}\, e^{-i\vec{r}\cdot\vec{k}} \psi_{1S}(r) \propto \exp\left(\frac{-\vec{k}^2}{2\alpha^2}\right). \tag{B2}$$

Employing the substitution ansatz [18, 33]:

$$\vec{k}_\perp \to \vec{k}_\perp, \qquad k_z \to (x - \bar{x})\frac{m_0}{2}, \qquad m_0^2 = \frac{m_c^2 + \vec{k}_\perp^2}{x\bar{x}}, \tag{B3}$$

where $\bar{x} = 1 - x$, and x is the longitudinal momentum fraction of the valence quark of the meson, the wave function can be taken as

$$\psi_{1S}(\vec{k}) \to \psi_{1S}(x, \vec{k}_\perp) \propto \exp\left(-\frac{(x - \bar{x})^2 m_c^2 + \vec{k}_\perp^2}{8\alpha^2 x\bar{x}}\right). \tag{B4}$$

Applying the Fourier transform to replace the transverse momentum $\vec{k}_\perp$ with its conjugate variable $\vec{b}$, the 1S-oscillator wave function can be taken as

$$\psi_{1S}(x, b) \sim \int \mathbf{d}^2\vec{k}_\perp e^{-i\vec{b}\cdot\vec{k}_\perp} \psi_{1S}(x, \vec{k}_\perp) \propto x\bar{x}\exp\left\{-\frac{m_c}{\omega}x\bar{x}\left[\left(\frac{x - \bar{x}}{2x\bar{x}}\right)^2 + \omega^2 b^2\right]\right\}. \tag{B5}$$

The modified wave functions can be written as

$$\psi_{X_{c\bar{c}}(1S)}(x, b) \propto \Phi^{\text{asy}}(x)\exp\left\{-\frac{m_c}{\omega}x\bar{x}\left[\left(\frac{x - \bar{x}}{2x\bar{x}}\right)^2 + \omega^2 b^2\right]\right\}, \tag{B6}$$

with $\Phi^{\text{asy}}(x)$ being set to the asymptotic models of the corresponding twists for light mesons, which have been given in [33]. Therefore, we can obtain the wave functions of the J/ψ and η_c mesons in Eq.(6) and Eq.(7)

$$\phi_\psi^L(x, b) = \frac{f_{J/\psi}}{2\sqrt{2N_c}}N_\psi^L x\bar{x}\exp\left\{-\frac{m_c}{\omega}x\bar{x}\left[\left(\frac{x - \bar{x}}{2x\bar{x}}\right)^2 + \omega^2 b^2\right]\right\}, \tag{B7}$$

$$\phi_\psi^t(x, b) = \frac{f_{J/\psi}}{2\sqrt{2N_c}}N_\psi^t (x - \bar{x})^2\exp\left\{-\frac{m_c}{\omega}x\bar{x}\left[\left(\frac{x - \bar{x}}{2x\bar{x}}\right)^2 + \omega^2 b^2\right]\right\}, \tag{B8}$$

$$\phi_{\eta_c}^v(x, b) = \frac{f_{\eta_c}}{2\sqrt{2N_c}}N_{\eta_c}^v x\bar{x}\exp\left\{-\frac{m_c}{\omega}x\bar{x}\left[\left(\frac{x - \bar{x}}{2x\bar{x}}\right)^2 + \omega^2 b^2\right]\right\}, \tag{B9}$$

$$\phi_{\eta_c}^s(x, b) = \frac{f_{\eta_c}}{2\sqrt{2N_c}}N_{\eta_c}^s\exp\left\{-\frac{m_c}{\omega}x\bar{x}\left[\left(\frac{x - \bar{x}}{2x\bar{x}}\right)^2 + \omega^2 b^2\right]\right\}, \tag{B10}$$

where N_c is the color number, $N_{\psi}^{L,t}$, $N_{\eta_c}^{v,s}$ are the normalization constants. All wave function in Eqs.(B7)-(B10) are symmetric under $x \leftrightarrow \bar{x}$ and normalized :

$$\int_0^1 \mathrm{d}x \; \phi_{\psi}^{L,t}(x,0) \;=\; \frac{f_{J/\psi}}{2\sqrt{2N_c}}, \tag{B11}$$

$$\int_0^1 \mathrm{d}x \; \phi_{\eta_c}^{v,s}(x,0) \;=\; \frac{f_{\eta_c}}{2\sqrt{2N_c}}. \tag{B12}$$

The parameter $\omega \approx m_{\psi(2S)} - m_{J/\psi(1S)} \approx m_{\eta_c(2S)} - m_{\eta_c(1S)} \approx 0.6$ GeV.

2. wave functions for Coulomb potential

In the static QCD potential, the interactions between heavy quarkonium can be parameterized and well described by a funnel shape Coulomb plus linear potential. At short distances one-gluon-exchange leads to the Coulomb-like potential with a strength proportional to the QCD coupling constant α_s [1]

$$V(r) = -C_F \frac{\alpha_s(r)}{r}, \tag{B13}$$

where $C_F = 4/3$ is the $SU(3)$ colour factor.

The radial wave function of the corresponding Schrödinger state is given by (note : the principle quantum number n associated with Coulomb potential is given by $n = (n_r - 1) + L + 1$)

$$\psi_{n_r L}(r) = \psi_{1S}(r) \propto \exp(-q_B r), \tag{B14}$$

where $q_B = C_F \mu_c \alpha_s$ is the Bohr momentum, $\mu_c = m_c/2$ is the reduced mass of the c-quark. Analogous to the treatment for the case of harmonic oscillator discussed above, we can get

$$\psi_{1S}(\vec{k}) \;\propto\; \frac{1}{(\vec{k}^2 + q_B^2)^2}, \tag{B15}$$

$$\psi_{1S}(x,b) \;\propto\; \frac{(x\bar{x})^2 m_c b}{\sqrt{1 - 4x\bar{x}(1-v^2)}} K_1(m_c b \sqrt{1 - 4x\bar{x}(1-v^2)}), \tag{B16}$$

where the typical velocity of the quarks in charmonium $v = q_B/m_c = 2\alpha_s/3 \sim 0.3$ [34]. The wave functions of the J/ψ and η_c mesons can be written as

$$\phi_{\psi}^L(x,b) \;=\; \frac{f_{J/\psi}}{2\sqrt{2N_c}} N_{\psi}^L \frac{(x\bar{x})^2 m_c b}{\sqrt{1 - 4x\bar{x}(1-v^2)}} K_1(m_c b \sqrt{1 - 4x\bar{x}(1-v^2)}), \tag{B17}$$

$$\phi_{\psi}^t(x,b) \;=\; \frac{f_{J/\psi}}{2\sqrt{2N_c}} N_{\psi}^t \frac{(x-\bar{x})^2 x\bar{x} m_c b}{\sqrt{1 - 4x\bar{x}(1-v^2)}} K_1(m_c b \sqrt{1 - 4x\bar{x}(1-v^2)}), \tag{B18}$$

$$\phi_{\eta_c}^v(x,b) = \frac{f_{\eta_c}}{2\sqrt{2N_c}} N_{\eta_c}^v \frac{(x\bar{x})^2 m_c b}{\sqrt{1-4x\bar{x}(1-v^2)}} K_1(m_c b\sqrt{1-4x\bar{x}(1-v^2)}), \qquad \text{(B19)}$$

$$\phi_{\eta_c}^s(x,b) = \frac{f_{\eta_c}}{2\sqrt{2N_c}} N_{\eta_c}^s \frac{x\bar{x} m_c b}{\sqrt{1-4x\bar{x}(1-v^2)}} K_1(m_c b\sqrt{1-4x\bar{x}(1-v^2)}). \qquad \text{(B20)}$$

The normalization conditions are the same as those of Eq.(B11) and Eq.(B12).

APPENDIX C: FORM FACTORS IN THE PERTURBATIVE QCD APPROACH

$$
\begin{aligned}
F_0^{B_c\to\eta_c} = {} & 8\pi m_{B_c}^2 C_F \int_0^1 \mathbf{d}x_1 \mathbf{d}x_2 \int_0^\infty b_2 \mathbf{d}b_2\, \phi_{B_c}(x_1) \\
& \times \Big\{ E_a(t_a)\alpha_s(t_a) H_a(\alpha,\beta_a,b_2)\Big[r_{\eta_c}\Big(2(1-x_2)-r_b\Big)\phi_{\eta_c}^s(x_2,b_2) \\
& \hspace{4cm} -\Big((1-x_2)-2r_b\Big)\phi_{\eta_c}^v(x_2,b_2)\Big] \\
& -E_b(t_b)\alpha_s(t_b) H_b(\alpha,\beta_b,b_2)\Big[\Big(r_{\eta_c}^2(1-x_1)+r_c\Big)\phi_{\eta_c}^v(x_2,b_2) \\
& \hspace{4cm} - 2r_{\eta_c}\Big((1-x_1)+r_c\Big)\phi_{\eta_c}^s(x_2,b_2)\Big]\Big\},
\end{aligned} \qquad \text{(C1)}
$$

$$
\begin{aligned}
\frac{m_{B_c}+m_{J/\psi}}{2m_{J/\psi}} A_1^{B_c\to J/\psi} = {} & -4\pi m_{B_c}^2 C_F \int_0^1 \mathbf{d}x_1 \mathbf{d}x_2 \int_0^\infty b_2 \mathbf{d}b_2\, \phi_{B_c}(x_1) \\
& \times \Big\{ E_a(t_a)\alpha_s(t_a) H_a(\alpha,\beta_a,b_2)\Big[\Big(2-x_2-4r_b-x_2 r_\psi^2\Big)\phi_\psi^L(x_2,b_2) \\
& \hspace{2.5cm} + \Big(r_b r_\psi - 2r_\psi + 4x_2 r_\psi + \frac{r_b}{r_\psi} - \frac{2}{r_\psi}\Big)\phi_\psi^t(x_2,b_2)\Big] \\
& -E_b(t_b)\alpha_s(t_b) H_b(\alpha,\beta_b,b_2)\Big(1+2r_c-2x_1+r_\psi^2\Big)\phi_\psi^L(x_2,b_2)\Big\},
\end{aligned} \qquad \text{(C2)}
$$

$$
\begin{aligned}
\frac{m_{B_c}-m_{J/\psi}}{-2m_{J/\psi}} A_2^{B_c\to J/\psi} = {} & -4\pi m_{B_c}^2 C_F \int_0^1 \mathbf{d}x_1 \mathbf{d}x_2 \int_0^\infty b_2 \mathbf{d}b_2\, \phi_{B_c}(x_1) \\
& \times \Big\{ E_a(t_a)\alpha_s(t_a) H_a(\alpha,\beta_a,b_2)\Big[\Big(-x_2+x_2 r_\psi^2\Big)\phi_\psi^L(x_2,b_2) \\
& \hspace{2.5cm} + \Big(r_b r_\psi - 2r_\psi - \frac{r_b}{r_\psi} + \frac{2}{r_\psi}\Big)\phi_\psi^t(x_2,b_2)\Big] \\
& +E_b(t_b)\alpha_s(t_b) H_b(\alpha,\beta_b,b_2)(1-2x_1)(1-r_\psi^2)\phi_\psi^L(x_2,b_2)\Big\},
\end{aligned} \qquad \text{(C3)}
$$

where $t_{a(b)} = \max(\sqrt{|\alpha|}, \sqrt{|\beta_{a(b)}|}, 1/b_2)$, $E_{a(b)}(t) = e^{-S_\psi(t)}$,

$$\alpha = -m_{B_c}^2(x_1-x_2)(x_1-r_\psi^2 x_2), \qquad \text{(C4)}$$

$$\beta_a = -m_{B_c}^2[(1-x_2)(1-r_\psi^2 x_2) - r_b^2], \qquad \text{(C5)}$$

$$\beta_b = -m_{B_c}^2[(1-x_1)(r_\psi^2 - x_1) - r_c^2], \qquad \text{(C6)}$$

$$S_\psi(t) = s(x_2 p_2^+, b_2) + s(\bar{x}_2 p_2^+, b_2) + 2\int_{1/b_2}^t \frac{\mathbf{d}\mu}{\mu}\gamma_q. \qquad \text{(C7)}$$

14

The quark anomalous dimension $\gamma_q = -\alpha_s/\pi$. The explicit expression of $s(Q,b)$ appearing in Sudakov form factor can be found in [35]. The hard functions H are

$$H_a(\alpha, \beta, b) = \frac{K_0(b\sqrt{\alpha}) - K_0(b\sqrt{\beta})}{\beta - \alpha}, \tag{C8}$$

$$H_b(\alpha, \beta, b) = \frac{K_0(b\sqrt{\alpha})}{\beta}. \tag{C9}$$

APPENDIX D: THE DECAY AMPLITUDES

1. The amplitudes for $B_c \to J/\psi\pi$ decay with the perturbative QCD approach

$$\begin{aligned}
\mathcal{A}_{\mathrm{FIG.3(a)}} = \; & 8\pi C_F f_\pi m_{B_c}^4 (1 - r_\psi^2) \int_0^1 \mathbf{d}x_1 \mathbf{d}x_2 \int_0^\infty b_2 \mathbf{d}b_2 \; \phi_{B_c}(x_1) E_a(t_a) \\
& \times \; \alpha_s(t_a) C_a(t_a) H_a(\alpha, \beta_a, b_2) \Big\{ r_\psi [2(1 - x_2) - r_b] \phi_\psi^t(x_2, b_2) \\
& \hspace{4cm} - [(1 - x_2) - 2r_b] \phi_\psi^L(x_2, b_2) \Big\},
\end{aligned} \tag{D1}$$

$$\begin{aligned}
\mathcal{A}_{\mathrm{FIG.3(b)}} = \; & 8\pi C_F f_\pi m_{B_c}^4 (1 - r_\psi^2) \int_0^1 \mathbf{d}x_1 \mathbf{d}x_2 \int_0^\infty b_2 \mathbf{d}b_2 \; \phi_{B_c}(x_1) E_b(t_b) \\
& \times \; \alpha_s(t_b) C_b(t_b) H_b(\alpha, \beta_b, b_2) \Big\{ r_\psi^2 (1 - x_1) + r_c \Big\} \phi_\psi^L(x_2, b_2),
\end{aligned} \tag{D2}$$

$$\begin{aligned}
\mathcal{A}_{\mathrm{FIG.3(c)}} = \; & \frac{32\pi C_F}{\sqrt{2N_c}} m_{B_c}^4 (1 - r_\psi^2) \int_0^1 \mathbf{d}x_1 \mathbf{d}x_2 \mathbf{d}x_3 \int_0^\infty b_2 \mathbf{d}b_2 \, b_3 \mathbf{d}b_3 \; \phi_{B_c}(x_1) \phi_\pi^a(x_3) \\
& \times \; E_c(t_c) \alpha_s(t_c) C_c(t_c) H_c(\alpha, \beta_c, b_2, b_3) \Big\{ r_\psi (x_1 - x_2) \phi_\psi^t(x_2, b_2) \\
& \hspace{4cm} + (1 - r_\psi^2)(x_1 - x_3) \phi_\psi^L(x_2, b_2) \Big\},
\end{aligned} \tag{D3}$$

$$\begin{aligned}
\mathcal{A}_{\mathrm{FIG.3(d)}} = \; & \frac{32\pi C_F}{\sqrt{2N_c}} m_{B_c}^4 (1 - r_\psi^2) \int_0^1 \mathbf{d}x_1 \mathbf{d}x_2 \mathbf{d}x_3 \int_0^\infty b_2 \mathbf{d}b_2 \, b_3 \mathbf{d}b_3 \; \phi_{B_c}(x_1) \phi_\pi^a(x_3) \\
& \times \; E_d(t_d) \alpha_s(t_d) C_d(t_d) H_d(\alpha, \beta_d, b_2, b_3) \Big\{ r_\psi (x_1 - x_2) \phi_\psi^t(x_2, b_2) \\
& \hspace{3cm} + [2(x_2 - x_1) - (x_2 - \bar{x}_3)(1 - r_\psi^2)] \phi_\psi^L(x_2, b_2) \Big\},
\end{aligned} \tag{D4}$$

where $t_{c(d)} = \max(\sqrt{|\alpha|}, \sqrt{|\beta_{c(d)}|}, 1/b_2, 1/b_3)$, $E_{c(d)}(t) = e^{-S_\psi(t) - S_\pi(t)}$,

$$\beta_c = -m_{B_c}^2 (x_2 - x_1)[(x_2 - x_1) - (x_2 - x_3)(1 - r_\psi^2)], \tag{D5}$$

$$\beta_d = -m_{B_c}^2 (x_2 - x_1)[(x_2 - x_1) - (x_2 - \bar{x}_3)(1 - r_\psi^2)], \tag{D6}$$

$$S_\pi(t) = s(x_3 p_3^-, b_3) + s(\bar{x}_3 p_2^-, b_3) + 2 \int_{1/b_3}^t \frac{\mathbf{d}\mu}{\mu} \gamma_q, \tag{D7}$$

$$C_{a(b)} = C_1 + C_2/N_c, \qquad C_{c(d)} = C_2, \tag{D8}$$

15

$$H_{c(d)}(\alpha, \beta, b_2, b_3) = \left\{ \theta(b_2 - b_3) K_0(b_2\sqrt{\alpha}) I_0(b_3\sqrt{\alpha}) + (b_2 \leftrightarrow b_3) \right\}$$
$$\times \left\{ \theta(+\beta) K_0(b_3\sqrt{\beta}) + \frac{i\pi}{2}\theta(-\beta) H_0^{(1)}(b_3\sqrt{-\beta}) \right\}, \qquad (D9)$$

where $C_{1,2}$ are the Wilson coefficients. The definitions of other parameters are the same as those in APPENDIX C.

2. The amplitudes for $B_c \to \eta_c\pi$ decay with the perturbative QCD approach

$$\mathcal{A}_{\text{FIG.3}(a)} = +i8\pi C_F f_\pi m_{B_c}^4 (1 - r_{\eta_c}^2) \int_0^1 \mathbf{d}x_1 \mathbf{d}x_2 \int_0^\infty b_2 \mathbf{d}b_2 \, \phi_{B_c}(x_1) E_a(t_a)$$
$$\times \, \alpha_s(t_a) C_a(t_a) H_a(\alpha, \beta_a, b_2) \Big\{ r_{\eta_c}[2(1 - x_2) - r_b]\phi_{\eta_c}^s(x_2, b_2)$$
$$- [(1 - x_2) - 2r_b]\phi_{\eta_c}^v(x_2, b_2) \Big\}, \qquad (D10)$$

$$\mathcal{A}_{\text{FIG.3}(b)} = -i8\pi C_F f_\pi m_{B_c}^4 (1 - r_{\eta_c}^2) \int_0^1 \mathbf{d}x_1 \mathbf{d}x_2 \int_0^\infty b_2 \mathbf{d}b_2 \, \phi_{B_c}(x_1) E_b(t_b)$$
$$\times \, \alpha_s(t_b) C_b(t_b) H_b(\alpha, \beta_b, b_2) \Big\{ [r_{\eta_c}^2(1 - x_1) + r_c]\phi_{\eta_c}^v(x_2, b_2)$$
$$- 2r_{\eta_c}[(1 - x_1) + r_c]\phi_{\eta_c}^s(x_2, b_2) \Big\}, \qquad (D11)$$

$$\mathcal{A}_{\text{FIG.3}(c)} = \frac{-i32\pi C_F}{\sqrt{2N_c}} m_{B_c}^4 (1 - r_{\eta_c}^2) \int_0^1 \mathbf{d}x_1 \mathbf{d}x_2 \mathbf{d}x_3 \int_0^\infty b_2 \mathbf{d}b_2 \, b_3 \mathbf{d}b_3 \, \phi_{B_c}(x_1)\phi_\pi^a(x_3)$$
$$\times \, E_c(t_c)\alpha_s(t_c) C_c(t_c) H_c(\alpha, \beta_c, b_2, b_3) \Big\{ r_{\eta_c}(x_1 - x_2)\phi_{\eta_c}^s(x_2, b_2)$$
$$- [(1 - r_{\eta_c}^2)(x_1 - x_3) + 2r_{\eta_c}^2(x_1 - x_2)]\phi_{\eta_c}^v(x_2, b_2) \Big\}, \qquad (D12)$$

$$\mathcal{A}_{\text{FIG.3}(d)} = \frac{+i32\pi C_F}{\sqrt{2N_c}} m_{B_c}^4 (1 - r_{\eta_c}^2) \int_0^1 \mathbf{d}x_1 \mathbf{d}x_2 \mathbf{d}x_3 \int_0^\infty b_2 \mathbf{d}b_2 \, b_3 \mathbf{d}b_3 \, \phi_{B_c}(x_1)\phi_\pi^a(x_3)$$
$$\times \, E_d(t_d)\alpha_s(t_d) C_d(t_d) H_d(\alpha, \beta_d, b_2, b_3) \Big\{ r_{\eta_c}(x_1 - x_2)\phi_{\eta_c}^s(x_2, b_2)$$
$$+ [2(x_2 - x_1) - (x_2 - \bar{x}_3)(1 - r_{\eta_c}^2)]\phi_{\eta_c}^v(x_2, b_2) \Big\}. \qquad (D13)$$

Acknowledgments

Theoretical Physics, China (KITP) for their hospitality while this work was started.

[1] N. Brambilla, *et al.* (Quarkonium Working Group), CERN-2005-005, hep-ph/0412158.

[2] J. F. Sun, Y. L. Yang, W. J. Du, and H. L. Ma, Phys. Rev. **D77**, 114004 (2008); and the references of [4,5,11-37] therein.

[3] F. Abe, *et al.* (CDF Collaboration), Phys. Rev. **D58**, 112004 (1998); Phys. Rev. Lett. **81**, 2432 (1998).

[4] T. Aaltonen *et al.* (CDF Collaboration), Phys. Rev. Lett. **100**, 182002 (2008).

[5] V. M. Abazov *et al.* (D0 Collaboration), Phys. Rev. Lett. **101**, 012001 (2008).

[6] M. Beneke, G. Buchalla, M. Neubert and C. T. Sachrajda, Phys. Rev. Lett. **83**, 1914 (1999); Nucl. Phys. **B591**, 313 (2000).

[7] C. H. Chang, and H. N. Li, Phys. Rev. **D55**, 5577 (1997).

[8] T. W. Yeh, and H. N. Li, Phys. Rev. **D56**, 1615 (1997).

[9] Y. Y. Keum, H. N. Li, and A. I. Sanda, Phys. Lett. **B504**, 6 (2001); Phys. Rev. **D63**, 054008 (2001).

[10] C. W. Bauer, S. Fleming, D. Pirjol, I. W. Stewart, Phys. Rev. **D63**, 114020 (2001).

[11] C. W. Bauer, D. Pirjol, I. W. Stewart, Phys. Rev. **D65**, 054022 (2002).

[12] F. Feng, J. P. Ma, and Q. Wang, arXiv:0807.0296 [hep-ph]; arXiv:0808.4017 [hep-ph]; H. N. Li, arXiv:0808.1526 [hep-ph].

[13] For example, see the references of [4,5] in arXiv:0807.0296.

[14] M. Wirbel, B. Stech, and M. Bauer, Z. Phys. **C29**, 637 (1985); M. Bauer, B. Stech, and M. Wirbel, Z. Phys. **C34**, 103 (1987).

[15] R. H. Li, C. D. Lü and H. Zou, Phys. Rev. **D78**, 014018 (2008).

[16] G. P. Lepage, and S. J. Brodsky, Phys. Rev. **D22**, 2157 (1980).

[17] T. Kurimoto, H. N. Li, A. I. Sanda, Phys. Rev. **D65**, 014007 (2001).

[18] C. H. Chen, H. N. Li, Phys. Rev. **D71**, 114008 (2005).

[19] C. D. Lü, M. Z. Yang, Eur. Phys. J. **C28**, 515 (2003).

[20] C. Amsler, *et al.* (Particle Data Group), Phys. Lett. **B667**, 1 (2008).

[21] T. W. Chiu, T. H. Hsien (TWQCD Collaboration), PoS. **LAT2006**, 180 (2007).

[22] D. Du, Z. Wang, Phys. Rev. **D39**, 1342 (1989).

[23] P. Colangelo, G. Nardulli, N. Paver, Z. Phys. **C57**, 43 (1993).

[24] V. V. Kiselev, A. Tkabladze, Phys. Rev. **D48**, 5208 (1993).

[25] V. V. Kiselev, A. K. Likhoded, A. I. Onishchenko, Nucl. Phys. **B569**, 473 (2000); Phys. Atom. Nucl. **63**, 2123 (2000).

[26] M. A. Ivanov, J. G. Kömer, P. Santorelli, Phys. Rev. **D63**, 074010 (2001)

[27] D. Ebert, R. N. Faustov, V. O. Galkin, Phys. Rev. **D68**, 094020 (2003).

[28] M. A. Ivanov, J. G. Kömer, P. Santorelli, Phys. Rev. **D71**, 094006 (2005).

[29] E. Hernández, J. Nieves, J. M. Verde-Velasco, Phys. Rev. **D74**, 074008 (2006).

[30] T. Huang, F. Zuo, Eur. Phys. J. **C51**, 833 (2007).

[31] W. Wang, Y. L. Shen, C. D. Lü, Eur. Phys. J. **C51**, 841 (2007).

[32] W. Wang, Y. L. Shen, C. D. Lü, arXiv:0811.3748 [hep-ph].

[33] A. E. Bondar, V. L. Chernyak, Phys. Lett. **B612**, 215 (2005).

[34] I. F. Allison, *et al.* (HPQCD, FNAL lattice and UKQCD Collaboration), Nucl. Phys. (Proc. Suppl.) **B140**, 440 (2005).

[35] Z. T. Wei, M. Z. Yang, Nucl. Phys. **B642**, 263 (2002).

[36] L.B. Guo, D. S. Du, Chin. Phys. Lett. **18**, 498 (2001).

[37] C. H. Chang, Y. Q. Chen, Phys. Rev. **D49**, 3399 (1994).

[38] M. A. Sanchis-Lozano, Nucl. Phys. **B440**, 251 (1995).

[39] P. Colangelo, F. D. Fazio, Phys. Rev. **D61**, 034012 (2000).

[40] R. C. Verma, A. Sharma, Phys. Rev. **D65**, 114007 (2002).

[41] V. V. Kiselev, hep-ph/0211021.

[42] J. F. Sun, G. F. Xue, Y. L. Yang, G. R. Lu, D. S. Du, Phys. Rev. **D77**, 074013 (2008).

[43] M. A. Ivanov, J. G. Körner, P. Santorelli, Phys. Rev. **D73**, 054024 (2006).

TABLE I: Form factors of $F_0^{B_c \to \eta_c}$ and $A_{0,1,2}^{B_c \to J/\psi}$

	$F_0^{B_c \to \eta_c}$	$A_0^{B_c \to J/\psi}$	$A_1^{B_c \to J/\psi}$	$A_2^{B_c \to J/\psi}$
$\omega = 0.5$ GeV	0.790	0.775	0.671	0.469
$\omega = 0.6$ GeV	0.741	0.730	0.636	0.454
$\omega = 0.7$ GeV	0.698	0.690	0.605	0.440
$\omega = 0.8$ GeV	0.660	0.655	0.578	0.427
$v = 0.25$	0.903	0.891	0.712	0.363
$v = 0.30$	0.824	0.819	0.664	0.364
$v = 0.35$	0.760	0.759	0.624	0.361
$v = 0.40$	0.705	0.708	0.589	0.356
[22]	$0.170 \sim 0.687$	$0.156 \sim 0.684$	$0.156 \sim 0.745$	$0.156 \sim 0.862$
[23]	0.20 ± 0.02	0.26 ± 0.07	0.27 ± 0.03	0.28 ± 0.09
[24]	0.23 ± 0.01	0.21 ± 0.03	0.21 ± 0.02	0.22 ± 0.02
[25]	0.66	0.60	0.63	0.69
[26]	0.76	0.69	0.68	0.66
[27]	0.47	0.40	0.50	0.73
[28]	0.61	0.56	0.56	0.54
[29]	0.49	0.45	0.49	0.56
[30]	0.87	0.27	0.75	1.69
[31]	——	$0.57^{+0.01}_{-0.02}$	$0.55^{+0.01}_{-0.03}$	$0.51^{+0.03}_{-0.04}$
[32]	$0.61^{+0.01+0.03}_{-0.02-0.04}$	0.53 ± 0.01	$0.50^{+0.01}_{-0.02}$	$0.44^{+0.02}_{-0.03}$

TABLE II: Amplitudes and branching ratio for $B_c \to J/\psi\pi$ decay, where δ is the strong phase.

	$\mathcal{A}_{\text{FIG.3(a)}}$	$\mathcal{A}_{\text{FIG.3(b)}}$	$\mathcal{A}_{\text{FIG.3(c)}}$ $[\delta]$	$\mathcal{A}_{\text{FIG.3(d)}}$ $[\delta]$	$\mathcal{BR}(B_c \to J/\psi\pi)$
$\omega = 0.5$ GeV	1.359	1.831	$-0.115 + i0.269$ $[113°]$	$+0.132 - i0.285$ $[-65°]$	1.913×10^{-3}
$\omega = 0.6$ GeV	1.235	1.767	$-0.103 + i0.267$ $[111°]$	$+0.115 - i0.285$ $[-68°]$	1.689×10^{-3}
$\omega = 0.7$ GeV	1.133	1.704	$-0.093 + i0.261$ $[110°]$	$+0.101 - i0.279$ $[-70°]$	1.506×10^{-3}
$\omega = 0.8$ GeV	1.049	1.643	$-0.086 + i0.253$ $[109°]$	$+0.090 - i0.271$ $[-72°]$	1.352×10^{-3}
$v = 0.25$	1.941	1.738	$-0.140 + i0.150$ $[133°]$	$+0.157 - i0.192$ $[-51°]$	2.542×10^{-3}
$v = 0.30$	1.692	1.686	$-0.130 + i0.162$ $[129°]$	$+0.144 - i0.203$ $[-55°]$	2.140×10^{-3}
$v = 0.35$	1.498	1.632	$-0.121 + i0.169$ $[126°]$	$+0.130 - i0.209$ $[-58°]$	1.834×10^{-3}
$v = 0.40$	1.342	1.576	$-0.111 + i0.174$ $[123°]$	$+0.118 - i0.212$ $[-61°]$	1.591×10^{-3}

TABLE III: Amplitudes and branching ratio for $B_c \to \eta_c\pi$ decay, where δ is the strong phase.

	$-i\mathcal{A}_{\text{FIG.3(a)}}$	$-i\mathcal{A}_{\text{FIG.3(b)}}$	$-i\mathcal{A}_{\text{FIG.3(c)}}$ $[\delta]$	$-i\mathcal{A}_{\text{FIG.3(d)}}$ $[\delta]$	$\mathcal{BR}(B_c \to \eta_c\pi)$
$\omega = 0.5$ GeV	1.490	1.828	$-0.112 + i0.211$ $[118°]$	$+0.127 - i0.300$ $[-67°]$	2.117×10^{-3}
$\omega = 0.6$ GeV	1.353	1.756	$-0.098 + i0.214$ $[115°]$	$+0.112 - i0.299$ $[-69°]$	1.858×10^{-3}
$\omega = 0.7$ GeV	1.242	1.685	$-0.087 + i0.212$ $[112°]$	$+0.100 - i0.292$ $[-71°]$	1.646×10^{-3}
$\omega = 0.8$ GeV	1.149	1.617	$-0.078 + i0.207$ $[111°]$	$+0.089 - i0.283$ $[-73°]$	1.470×10^{-3}
$v = 0.25$	2.140	1.665	$-0.131 + i0.104$ $[141°]$	$+0.154 - i0.189$ $[-51°]$	2.792×10^{-3}
$v = 0.30$	1.864	1.608	$-0.121 + i0.119$ $[135°]$	$+0.141 - i0.201$ $[-55°]$	2.323×10^{-3}
$v = 0.35$	1.649	1.548	$-0.112 + i0.129$ $[131°]$	$+0.129 - i0.208$ $[-58°]$	1.970×10^{-3}
$v = 0.40$	1.476	1.488	$-0.102 + i0.137$ $[127°]$	$+0.118 - i0.212$ $[-61°]$	1.692×10^{-3}

TABLE IV: Branching ratio for $B_c \to J/\psi\pi$, $\eta_c\pi$ decay in previous works (in the unit of 10^{-3}).

$\mathcal{BR}(B_c \to \eta_c\pi)$	0.13~1.55 [22]	0.85 [27]	0.94 [29]	1.44~2.46 [36]	2.30 [37]	1.8 [38]
	0.26 [39]	9.30 [40]	2.00 [41]	1.16~1.34 [42]	1.90 [43]	
$\mathcal{BR}(B_c \to J/\psi\pi)$	0.02~0.34 [22]	0.61 [27]	0.76 [29]	$2.0^{+0.8+0.0}_{-0.7-0.1}$ [31]	2.19 [37]	1.7 [38]
	1.30 [39]	4.50 [40]	1.30 [41]	1.08~1.24 [42]	1.70 [43]	

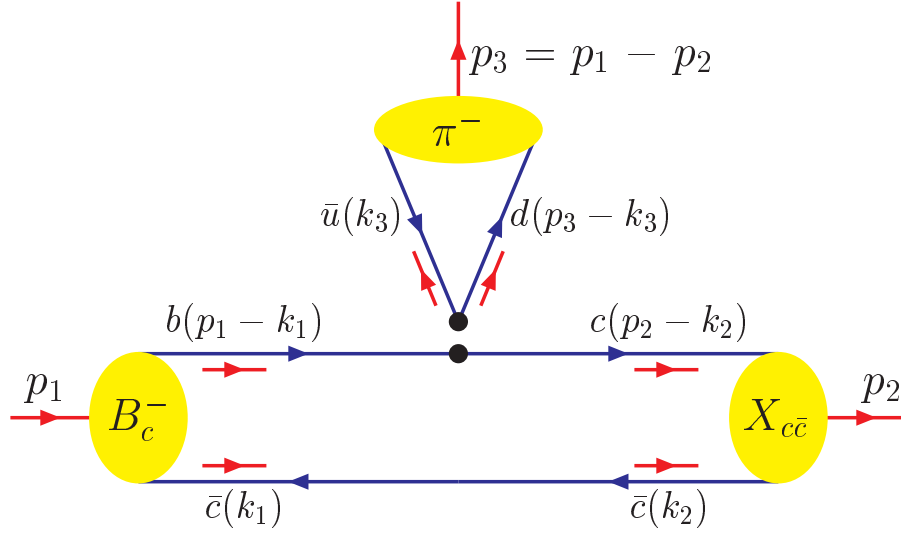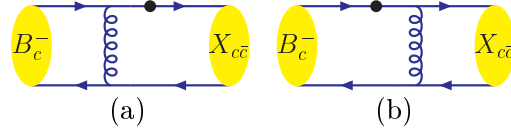FIG. 1: Kinematic variables for $B_c^- \to X_{c\bar{c}}\pi^-$ decays.

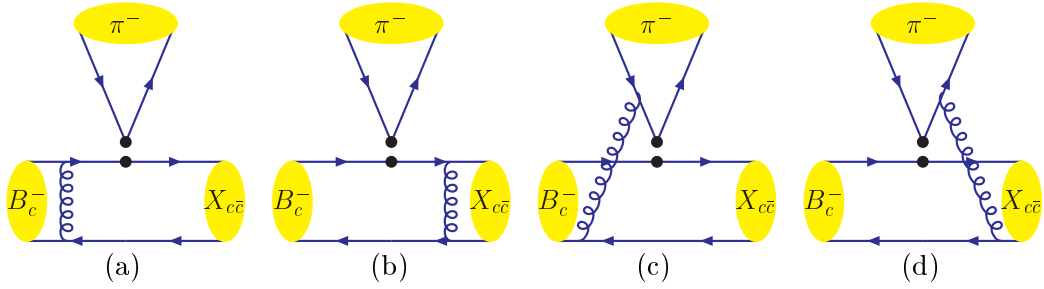FIG. 2: Feynman diagrams contributing to the $B_c \to X_{c\bar{c}}$ form factors.

FIG. 3: Feynman diagrams for $B_c^- \to X_{c\bar{c}}\pi^-$ decays.

21